Vibrational properties of (R)methylthiirane from Mo/ller–Plesset perturbation theory

Roger D. Amos, Nicholas C. Handy, and Paolo Palmieri

Articles you may be interested in

Mo/ller–Plesset perturbation theory applied to vibrational problems
J. Chem. Phys. **105**, 11261 (1996); 10.1063/1.472922

Surprising cases of divergent behavior in Mo/ller–Plesset perturbation theory
J. Chem. Phys. **105**, 5082 (1996); 10.1063/1.472352

Pseudospectral Mo/ller–Plesset perturbation theory through third order
J. Chem. Phys. **100**, 3631 (1994); 10.1063/1.466350

Frequencydependent hyperpolarizabilities in the Mo/ller–Plesset perturbation theory
J. Chem. Phys. **99**, 3779 (1993); 10.1063/1.466124

Laplace transform techniques in Mo/ller–Plesset perturbation theory
J. Chem. Phys. **96**, 489 (1992); 10.1063/1.462485

Vibrational properties of (R)-methylthiirane from Møller–Plesset perturbation theory

Roger D. Amos and Nicholas C. Handy
University Chemical Laboratory, Lensfield Road, Cambridge CB2 1EW, United Kingdom

Paolo Palmieri
Dipartimento di Chimica Fisica ed Inorganica, Viale Risorgimento 4, 40136 Bologna, Italy

The infrared, Raman frequencies and intensities and the vibrational dichroism of the molecule have been computed using Hartree–Fock and Møller–Plesset perturbation theories. In general, the frequencies and intensities computed by perturbation theory improve the Hartree–Fock description of the spectra. For one of the spectral regions, only the values corrected by perturbation theory are entirely compatible with the measured intensities and signs.

I. INTRODUCTION

The important operation to be performed to study theoretically molecular vibrational properties is the evaluation of molecular energy and property derivatives with respect to the nuclear coordinates. The energy gradient $\partial E/\partial Q_i$ and higher-order derivatives $\partial^2 E/\partial Q_i \partial Q_j$ allow the determination of the theoretical molecular equilibrium geometry, the force fields, and the normal modes Q_i. The dipole $\partial\mu/\partial Q_i$ and the polarizability derivatives $\partial\alpha/\partial Q_i$ give the intensities of the vibrational transitions in the harmonic approximation. In particular, the dipole strength for the fundamental vibrational transition from the ground $|0\rangle$ to the lowest excited $|1\rangle$ state is defined[1]

$$D_i = \left\langle \frac{\partial\mu}{\partial Q_i} \left| \frac{\partial\mu}{\partial Q_i} \right\rangle \langle 0|Q_i|1\rangle^2 \right. \tag{1}$$

and the differential Raman cross sections for polarized σ_i^P and for depolarized light σ_i^D are, respectively,[2]

$$\sigma_i^P = \left[45\left(\frac{\partial\alpha^{iso}}{\partial Q_i}\right)^2 + 4\left(\frac{\partial\alpha^{aniso}}{\partial Q_i}\right)^2 \right]\langle 0|Q_i|1\rangle^2, \tag{2}$$

$$\sigma_i^D = 3\left(\frac{\partial\alpha^{aniso}}{\partial Q_i}\right)^2 \langle 0|Q_i|1\rangle^2. \tag{3}$$

Similarly, for optically active molecules, the dichroism of the fundamental transition is given by the rotational strength R_i (Ref. 3)

$$R_i = \mathscr{I}\left(\left\langle \frac{\partial\mu}{\partial Q_i} \left| \frac{\partial m}{\partial \dot{Q}_i} \right\rangle \langle 0|Q_i|1\rangle\langle 1|\dot{Q}_i|0\rangle \right. \right). \tag{4}$$

The new type of derivative that appears in this case, $\partial m/\partial \dot{Q}_i$, the magnetic dipole derivative with respect to the nuclear velocity $\dot{Q}_i$ (see Refs. 4 and 5), is easily factorized into products of wave function derivatives as recently discussed by Stephens[6] and Buckingham,[5] and its evaluation does not pose additional problems. There has been increased interest in the latter property due to recent advances in the instrumentation[3,7,8] and in the theory of vibrational circular dichroism (VCD).[3–6,9–17]

The evaluation of all these derivatives has now been efficiently implemented[18] and can be routinely performed at the self-consistent-field (SCF) level of description: For many molecules, a satisfactory description of the vibrational properties has been obtained.[19]

It has been recognized that the main limitation of this procedure comes from the approximate description of the normal modes Q_i but this can be improved by some empirical adjustment of the *ab initio* SCF force field.[20–22] This scaling seems to be particularly important for VCD which probes subtle details of the vibrational modes.[16]

Despite numerous successful applications of the procedure, the case of R-methylthiirane has been recently reported[23] where a scaled SCF force field adjusted with respect to infrared (IR) frequencies and IR and VCD intensities[24] is in the end unable to account for Raman

TABLE I. Computed frequencies $\bar{\nu}$ (cm^{-1}) and intensities for C–H stretching vibrations: dipole D_i(10^{-4}D^2) and rotational R_i(10^{-8} D^2)strengths with (a) distributed origin gauge and with common origin gauge at (b) the center of the mass and at (c) the sulphur atom. Dissymmetry factors $g_i(a) = 4R_i(a)/D_i$ computed with the distributed origin gauge and differential Raman cross sections σ_i^P, σ_i^D (Å^4/amu).

Q_i	$\bar{\nu}_i$	D_i	R_i(a)	R_i(b)	R_i(c)	$10^4 g_i$(a)	σ_i^P	σ_i^D
(CH$_3$)$_s$	3113	29.423	− 1.474	− 1.400	− 0.868	0.20	135.67	4.931
(CH$_2$)$_s$	3204	15.426	0.552	2.066	0.318	0.14	39.761	27.800
(CH$_3$)$_a$	3219	14.085	6.140	12.319	12.029	1.74	32.338	24.253
(CH$_3$)$_a$	3229	11.146	− 6.258	− 23.032	− 22.466	− 2.25	98.067	10.365
C*–H	3241	26.736	6.677	16.361	14.909	1.00	73.235	12.910
(CH$_2$)$_a$	3312	6.440	0.582	1.317	3.355	0.36	33.975	24.209

intensities in the congested region of the spectrum, where a large number of nearly degenerate fundamentals occur. There are in fact clear indications[25] that the scaling has in this case produced artifacts and incorrect expressions for some of the normal modes.

As normally applied, scaling must improve the agreement between the calculated frequencies and the observed fundamentals. However, it is the form of the normal modes that is of greatest importance for the prediction of intensities, and while the modes will sometimes be improved, there is no guarantee of this, as there are an infinite number of force constant matrices corresponding to a given set of frequencies.

In this article, we discuss all vibrational properties of this molecule using an alternative procedure: We avoid the scaling but improve the SCF description by including elec-
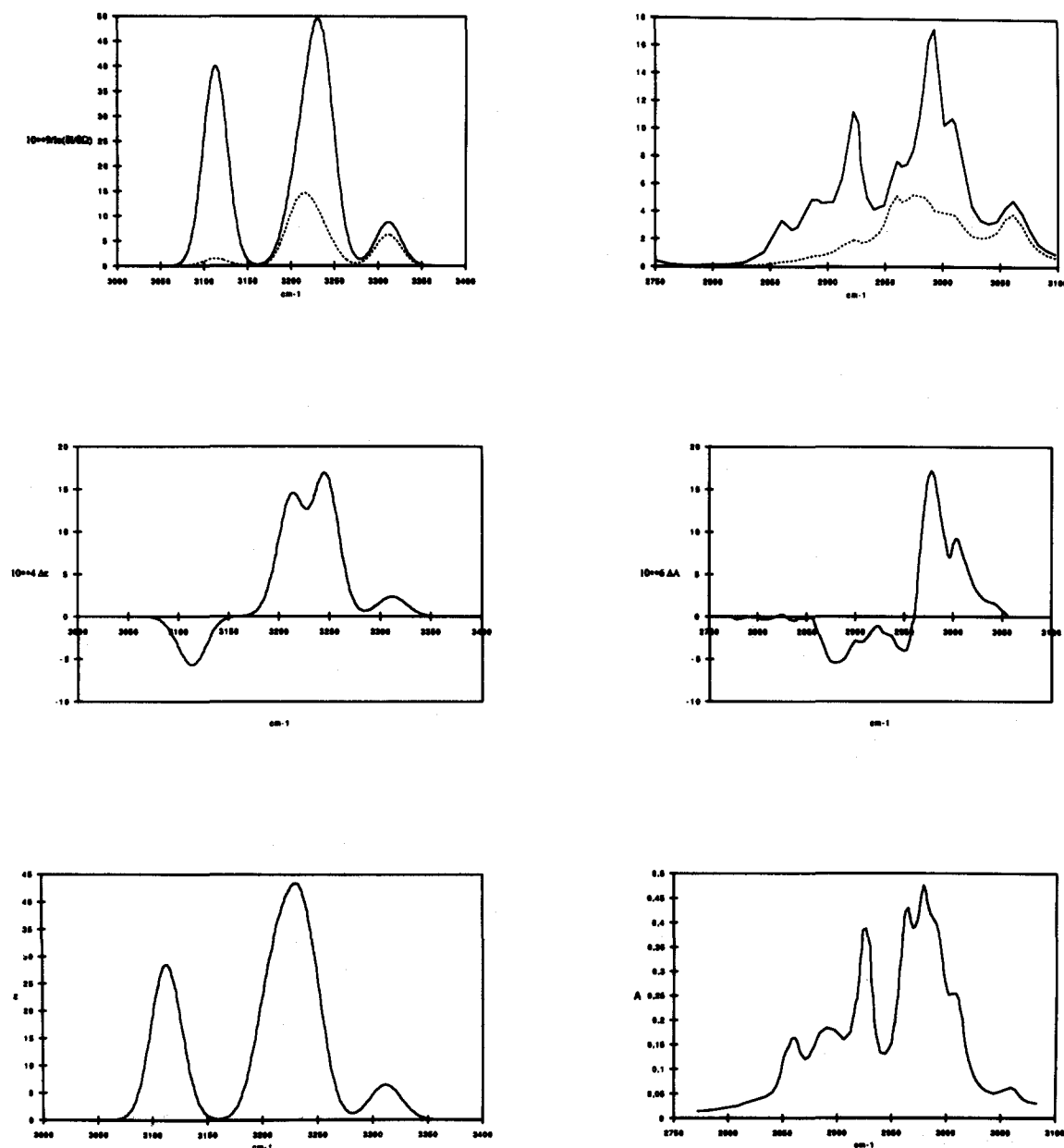

FIG. 1. Computed (left) and experimental (right) spectra of R-methylthiirane in the C–H stretching region: 2750–3100 cm^{-1} experimental and 3000–3400 cm^{-1} computed by the MP2 method and the distributed origin gauge for VCD intensities. IR (lower), VCD (middle), polarized (full line), and depolarized (dashed line) Raman spectra (upper). The scaling factors for the IR, VCD, and Raman intensities computed by Eqs. (5)–(7) are 1, 10^4, and 10^9, respectively; the experimental intensities from Ref. 23 are given in units of absorbance A (IR), 10^{-6} absorbance ΔA (VCD), and in arbitrary units (Raman).
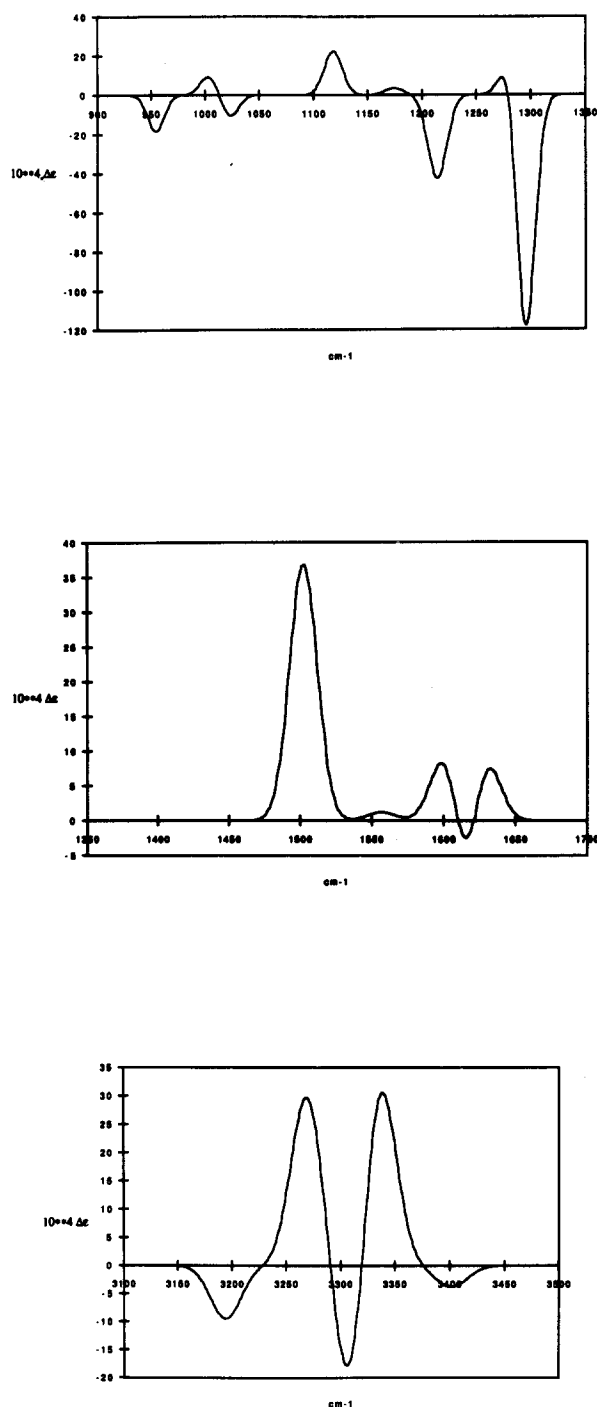
FIG. 2. VCD spectra computed by the SCF method: 3100—3500 cm^{-1} (lower), 1350–1700 cm^{-1} (middle), and 900–1350 cm^{-1} (upper). Gauge, units, and scaling factors as in Fig. 1.

tronic correlation effects, via the Møller–Plesset method to second order (MP2),[26,27] in the evaluation of the normal modes and of the dipole derivatives $\partial\mu/\partial Q_i$ (see Ref. 18). We keep the SCF description of the polarizabilities and magnetic dipole surfaces, for which efficient MP2 procedures have not yet been implemented.[18] Note that the frequencies we calculate are actually harmonic frequencies.

It will be shown that this procedure provides a very good description of all vibrational properties of methylthiirane and, therefore, can be recommended for similar studies on molecules of moderate complexity.

II. METHODS AND CALCULATIONS

Equilibrium geometry, harmonic force field, normal coordinates, and electric dipole derivatives have been evaluated by the SCF and MP2 methods using the CADPAC[28] suite of programs and a variety of basis sets from its library. These include Dunning's double zeta (DZP),[29] the 6-31G**,[30] and the 6-31G-extended[31] bases of contracted Gaussian orbitals, inclusive of polarization orbitals on heavy atoms and hydrogens. SCF polarizability and magnetic dipole derivatives have been evaluated using the normal coordinates from the SCF and the MP2 force fields. The intensities given by Eqs. (1)–(4) have been converted into spectral profiles. The IR absorption is defined by

$$\epsilon(\overline{v}) = A \sum_i Z_i^{-1} D_i \overline{v} \, f_i(\overline{v} - \overline{v}_i), \qquad (5)$$

where $Z_i = 1 - \exp(-hc\overline{v}_i/kT)$ is the vibrational partition function for mode i and $f_i(\overline{v} - \overline{v}_i)$ a line shape function, which was taken a normalized Gaussian, with bandwidth fixed to $\sqrt{\overline{v}_i}/4$ (see Refs. 32 and 33) for all bands. For the VCD spectrum, a similar expression applies:

$$\Delta\epsilon(\overline{v}) = 4A \sum_i Z_i^{-1} R_i \overline{v} \, f_i(\overline{v} - \overline{v}_i). \qquad (6)$$

As for all magnetic properties, the values of the magnetic factor in Eq. (2), and therefore the values of the rotational strengths, computed from approximated molecular wave functions are not invariant to a shift of the origin of the reference frame.[34,35] This dependence is generally tested by repeating the computations for reasonable choices of the gauge in the molecular region. Therefore, all rotational strengths have been computed using the distributed origin gauge and common origin gauges at the center of mass and at the sulphur atom.[34]

The Raman intensities were next obtained from the differential Raman cross sections

$$\frac{1}{I_0(\overline{v}_0)} \frac{\partial I^{P(D)}(\overline{v})}{\partial\Omega} = B \sum_i Z_i^{-1}(\overline{v} - \overline{v}_0)^4 \sigma_i^{P(D)} f_i$$

$$\times (\overline{v} - \overline{v}_i), \qquad (7)$$

defined as the scattered light power $I(\overline{v})$ per unit solid angle Ω per mole and per unit irradiance $I_0(\overline{v}_0)$ of the exciting laser radiation,[1] whose frequency $\overline{v}_0$ was set to 488 nm.[23,25] When all quantities are in cgs units, the constants A, B in Eqs. (5)–(7) take the values $A = (2\pi)^3(3hc1000 \ln 10)^{-1}L$ and $B = (2\pi)^4L/45$, L being the Avogadro number.

We did not observe significant changes in the computed spectral profiles with various basis sets and therefore only DZP results will be quoted and discussed in detail.

III. RESULTS AND DISCUSSION

Our discussion will be based on the comparison of the experimental and computed spectral profiles. To simplify the comparison, it is convenient to divide the spectra into

the following four spectral regions, which provide a rough classification of molecular vibrations.

A. The C–H stretching modes

The frequencies and the intensities computed for the C–H stretching modes are displayed in Table I. From these values the IR, VCD, and Raman spectra have been computed by Eqs. (5)–(7) and compared with experiment in Fig. 1.

In agreement with experiment, the first fundamental is strongly Raman polarized and has a small negative VCD; the last is Raman depolarized and has a small positive VCD. All remaining four fundamentals are computed to be nearly degenerate.

Due to the strong overlap of these bands, VCD is more informative than the IR and the Raman spectra in this region. The C*–H vibration carries the highest VCD intensity and, in agreement with perturbation theory,[36] the two $(CH_3)_a$ vibrations originate an intense VCD couplet with the positive component to lower frequencies. As seen by comparing the spectra in Figs. 1 and 2, these bands are well separated in the SCF description [see Fig. 2(a)] but the corresponding MP2 bands strongly overlap, leading to the cancellation of the negative component of the VCD couplet (see Fig. 1). We conclude that correlation affects frequencies more than intensities in this spectral region.

Due to the strong overlap of these bands, the comparison between the computed (Table I) and the experimental values[23] of the dissymmetry factors g_i do not provide additional information for assignment.

The overall intensity distribution in the three IR and Raman bands the signs, and the relative VCD intensities are, on the whole, reproduced apart from the small negative feature at 2920 (cm^{-1}) in the experimental VCD spectrum of Fig. 1. The latter is accounted for only by inverting the order of the two $(CH_3)_a$ degenerate components, leading to the VCD spectrum of Fig. 3, which nearly exactly mimics the overall profile of VCD in this region.

Contrary to the conclusions drawn in Ref. 24, we find that the signs of most VCD bands in this region are not modified by moving the origin of the reference frame when evaluating the magnetic factor in Eq. (4). As seen in Table I, where we compare the VCD rotational strengths evaluated for three different choices of the gauge, only for the least intense band of lowest frequency is the VCD sign inverted when we move the origin to the sulphur atom. The distributed origin gauge seems to provide a more realistic description of the VCD intensity distribution. This
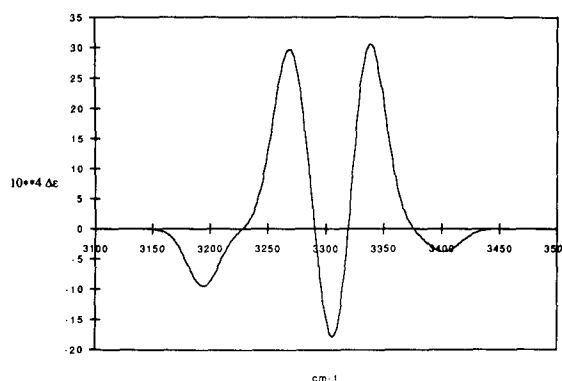

FIG. 3. The VCD spectrum of (R)-methylthiirane in the C–H stretching region obtained by inverting the order of the two nearly degenerate $(CH_3)_a$ MP2 frequencies. Gauge, units, and scaling factors as in Fig. 1.

result restores confidence in our predictions, and the assignments that emerge from these results are entirely consistent with those proposed in Ref. 23.

B. The (CH_3), (CH_2) deformation modes and the C*–H bending vibration

In Table II we list the dipole, rotational strengths and the differential Raman cross sections computed for these vibrational modes. By comparing the spectra in Fig. 4, a one-to-one correspondence is easily established between the computed and the experimental IR, Raman, and VCD peaks in the frequency range 1350–1460 cm^{-1}.

The IR and the Raman spectra are dominated by the intense absorption system at 1430–1450 cm^{-1} on the high-frequency side of the interval. Its composite structure is clear in the IR and Raman spectra and is well simulated in our spectra, where it encompasses the symmetric $(CH_2)_s$ and the two antisymmetric $(CH_3)_a$ deformations. These, in agreement with perturbation theory,[36] generate a VCD couplet of moderate intensity. Conversely, the intense positive band at 1346 cm^{-1}, which is mainly a C*–H bending mode in our description, is prominent in the VCD spectrum at the opposite side of the interval. The dissymetry factor computed for this band, 3.16×10^{-4}, well compares with the experimental value of 4.3×10^{-4}.[23] The intermediate band at 1380 cm^{-1} is assigned to the $(CH_3)_s$ deformation due to the good agreement between the experimental and the computed intensities. Signs and intensities

TABLE II. Computed frequencies $\bar{v}_i(cm^{-1})$ intensities for the (CH_3), (CH_2) deformation modes and for the C*–H bending vibration: Notation and units as in Table I.

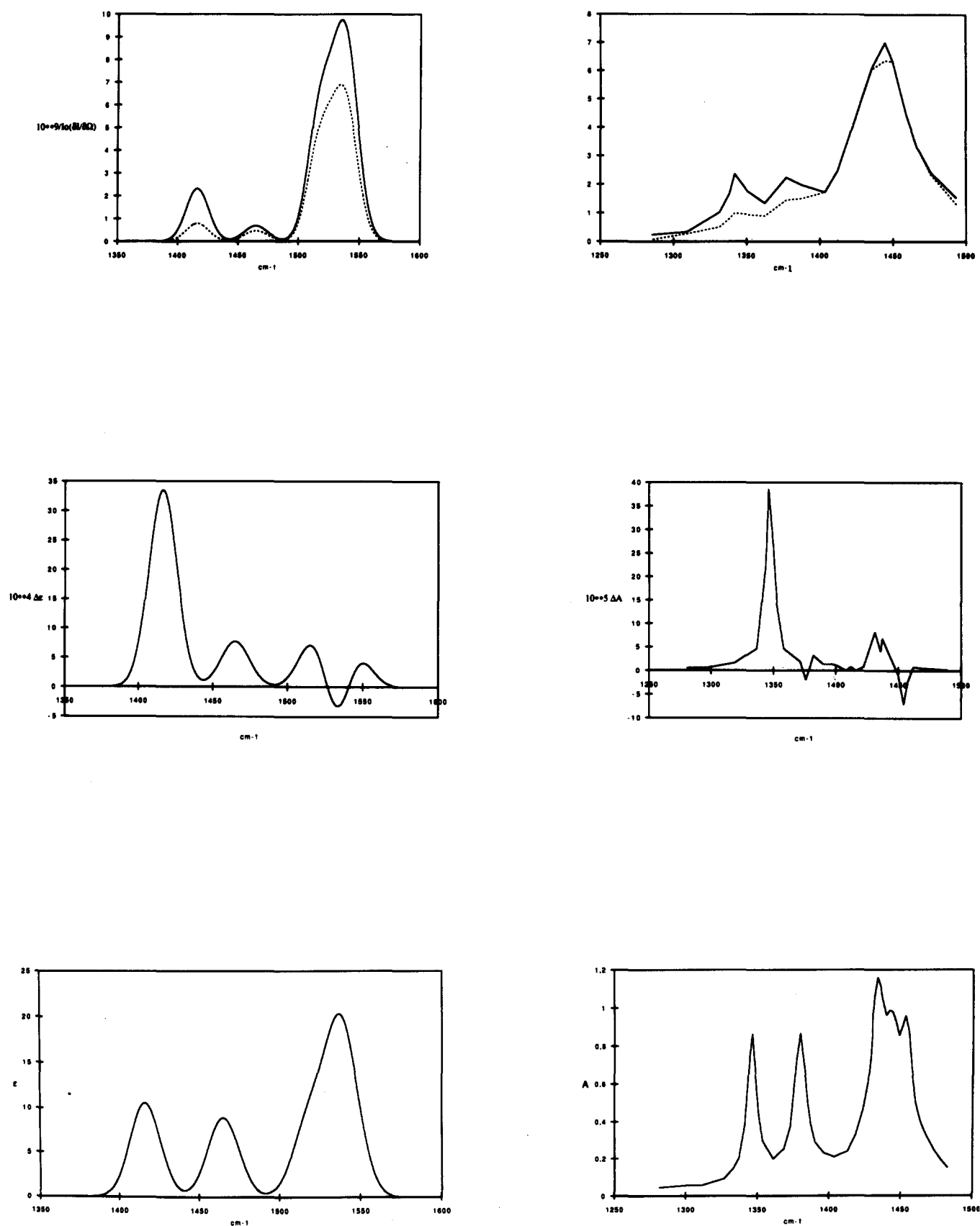| Q_i	$\bar{v}_i$	D_i	$R_i(a)$	$R_i(b)$	$R_i(c)$	$10^4 g_i(a)$	σ_i^p	σ_i^D
C*–H/CH$_3$	1416	16.168	12.791	12.200	13.054	3.16	1.660	0.566
$(CH_3)_s$	1465	13.429	2.879	2.717	0.891	0.86	0.517	0.346
$(CH_3)_a$	1518	11.859	3.143	4.271	5.022	1.06	4.688	3.511
$(CH_3)_a$	1536	20.523	− 5.084	− 3.605	− 5.461	− 0.99	5.433	4.019
$(CH_2)_s$	1543	9.030	4.410	5.758	5.662	1.95	2.326	1.328

FIG. 4. Experimental spectra (right) of R-methylthiirane in the 1250 to 1500-cm^{-1} region; the theoretical spectra (left) have been computed in the frequency interval 1350–1600 cm^{-1} by the MP2 method. IR (lower), VCD (middle), polarized (full line), and depolarized (dashed line) Raman spectra (upper). Gauge, scaling factors, and units for the theoretical intensities as in Fig. 1. The experimental intensities from Ref. 23 are given in units of absorbance A(IR), 10^{-5} absorbance ΔA (VCD), and in arbitrary units (Raman).

TABLE III. Computed frequencies $\bar{v}_i$ (cm^{-1}) and intensities for the remaining C–H deformation modes: Notation and units as in Table I.

Q_i	$\bar{v}_i$	D_i	$R_i(a)$	$R_i(b)$	$R_i(c)$	$10^4 g_i(a)$	σ_i^P	σ_i^D
CH$_2$/CH	924	11.017	−7.429	−0.772	−2.339	−2.70	11.976	2.927
(CH$_2$)$_t$	966	14.453	−0.913	−1.610	−10.413	−0.25	3.119	0.449
(CH$_2$)$_t$	977	7.558	−7.877	−8.488	−7.967	−4.17	2.401	1.466
CH/CH$_3$	1059	15.651	14.203	28.854	26.544	3.63	4.063	1.668
(CH$_2$)$_w$	1127	19.623	1.702	1.272	5.939	0.01	9.984	13.167
(CH$_2$)$_w$	1151	84.226	−20.220	−29.337	−34.929	−0.96	0.857	0.493
(CH$_2$)$_\tau$	1220	14.433	3.202	−0.449	1.4241	0.89	12.585	3.282
(CH$_2$)$_\tau$	1239	10.370	5.807	3.255	3.019	2.24	1.803	0.909

of VCD were found fairly constant with different choices of the gauge (see Table II).

As shown from the detailed comparison of the VCD spectra in Figs. 4 and 2(b), we confirm the SCF description of these modes and the assignments of Ref. 23.

C. The remaining C–H deformation modes

The frequencies of these modes and their intensities are listed in Table III and the computed spectral profiles are compared in Fig. 5 to the experimental spectra in the frequency interval 800–1300 cm^{-1}. This is the most congested region of the spectrum and different assignments of the absorptions in this interval have been proposed. The scaled *ab initio* force field by Alper *et al.*[24] explains only part of the observed VCD features while producing large fluctuations of signs and values of rotational strengths with the gauge (see Fig. 2 in Ref. 24). Moreover, this force field, which suffers not only for the limited basis set used in the computation but also for the lack of a proper geometry optimization, does not explain Raman intensities in this spectral region:[25] The two highest frequency bands are inverted and the intensities of the three lowest frequency bands are clearly incorrect. In this respect the unscaled *ab initio* SCF force field, producing the correct intensity ordering of the Raman bands, seems to be preferred, posing the problem of whether scaled or unscaled SCF *ab initio* force fields should be used for vibrational assignments.[25] Unfortunately SCF is in this case also inadequate and important discrepancies are noticed when the SCF VCD spectrum in Fig. 2(c) is compared to the experimental spectrum in Fig. 5. In particular, the highest frequency band is predicted to be very intense and negative compared with the positive weak feature at 1160 cm^{-1} in the experimental spectrum. Conversely, the intense negative VCD band at 1070 cm^{-1} is too weak in our simulated spectrum. It is interesting to notice that the two modes are coupled by the MP2 force field producing the right intensity for the lower frequency mode and reverting the sign of the higher frequency mode. Intensity redistribution is also observed on the low-frequency side of this spectral interval leading to a very good agreement between the experimental and simulated VCD spectra. Given this assignment, the dissymmetry factor 3.8×10^{-4} (see Ref. 23) of the band at 1007 cm^{-1}, which is resolved and prominent in the VCD spectrum of the neat liquid,[23] well compares with our com-

puted value of 3.63×10^{-4}. Raman intensities are also correctly predicted: In particular, the band at 865 cm^{-1} is computed to be very intense and polarized and the intensity ordering of the two high-frequency bands clearly reproduced in the simulated spectrum of Fig. 5. In conclusion, the MP2 force field accounts for all experimental information available from IR, Raman, and VCD spectroscopies in this frequency interval.

D. The low-frequency modes

The five vibrational modes in Table IV have been assigned to the frequency range 600–200 cm^{-1}. Experimental VCD intensities are not available in this region. Two very intense bands at 592 and 622 cm^{-1} dominate the Raman spectrum with the first peak highly polarized. These two bands have been assigned to the two ring modes, which fits very well with our computed Raman intensities and polarization ratios (see Fig. 6). The corresponding VCD couplet is easily explained by perturbation theory as discussed in Ref. 36 for the methyl deformation modes. The assignment of all remaining bands in this region is also confirmed.

IV. CONCLUSIONS

The title molecule has been studied by the SCF and the MP2 methods to obtain normal modes and IR, Raman, and VCD frequencies and intensities for all vibrations. Inclusion of correlation effects improves the theoretical predictions and, apart the inversion of the two degenerate (CH$_3$)$_a$ stretching modes, all important spectral features in the four regions of the spectra are explained. In particular, the assignment of the C–H stretching vibrations, the CH$_3$, CH$_2$ deformation, and the C*–H bending modes is confirmed.

The MP2 force field and dipole derivatives provide the only description of the third region of the spectrum, which is compatible with the measured IR, Raman, and VCD intensities. The signs, if not the absolute values, of VCD intensities are nearly always unaffected by the choice of the gauge. The present approach, although computationally demanding, seems practical for molecules of moderate complexity.
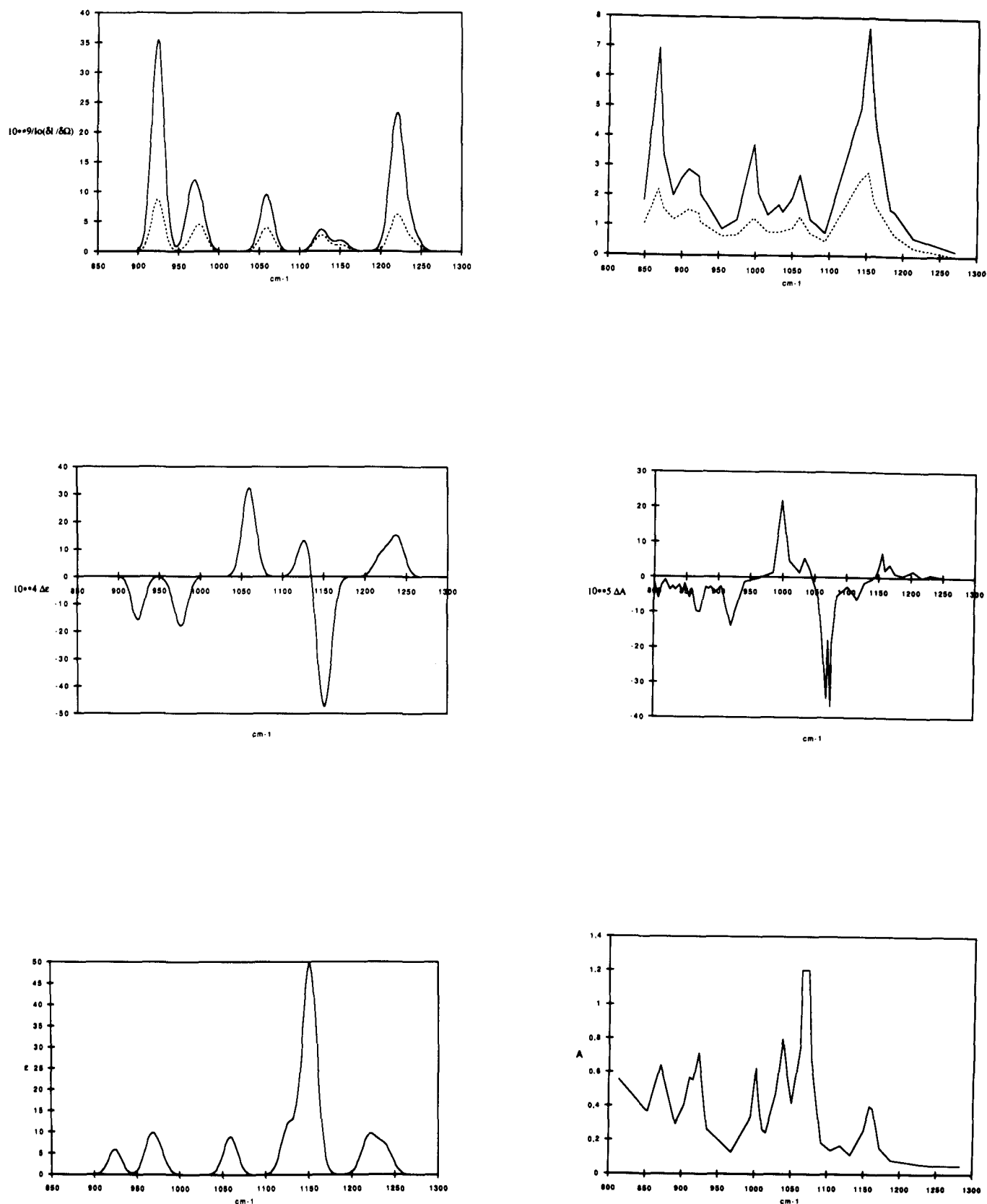
FIG. 5. Experimental spectra (right) of R-methylthiirane in the 800- to 1300-cm^{-1} region; the theoretical spectra (left) have been computed in the frequency interval 850–1300 cm^{-1} by the MP2 method. IR (lower), VCD (middle), polarized (full line), and depolarized (dashed line) Raman spectra (upper). Gauge, scaling factors, and units for the theoretical intensities as in Fig.1. The experimental intensities from Ref. 23 are given in units of absorbance A (IR), 10^{-5} absorbance ΔA (VCD), and in arbitrary units (Raman).

TABLE IV. Computed frequencies $\bar{v}_i$(cm^{-1}) and intensities for the low-frequency modes: Notation and units as in Table I.

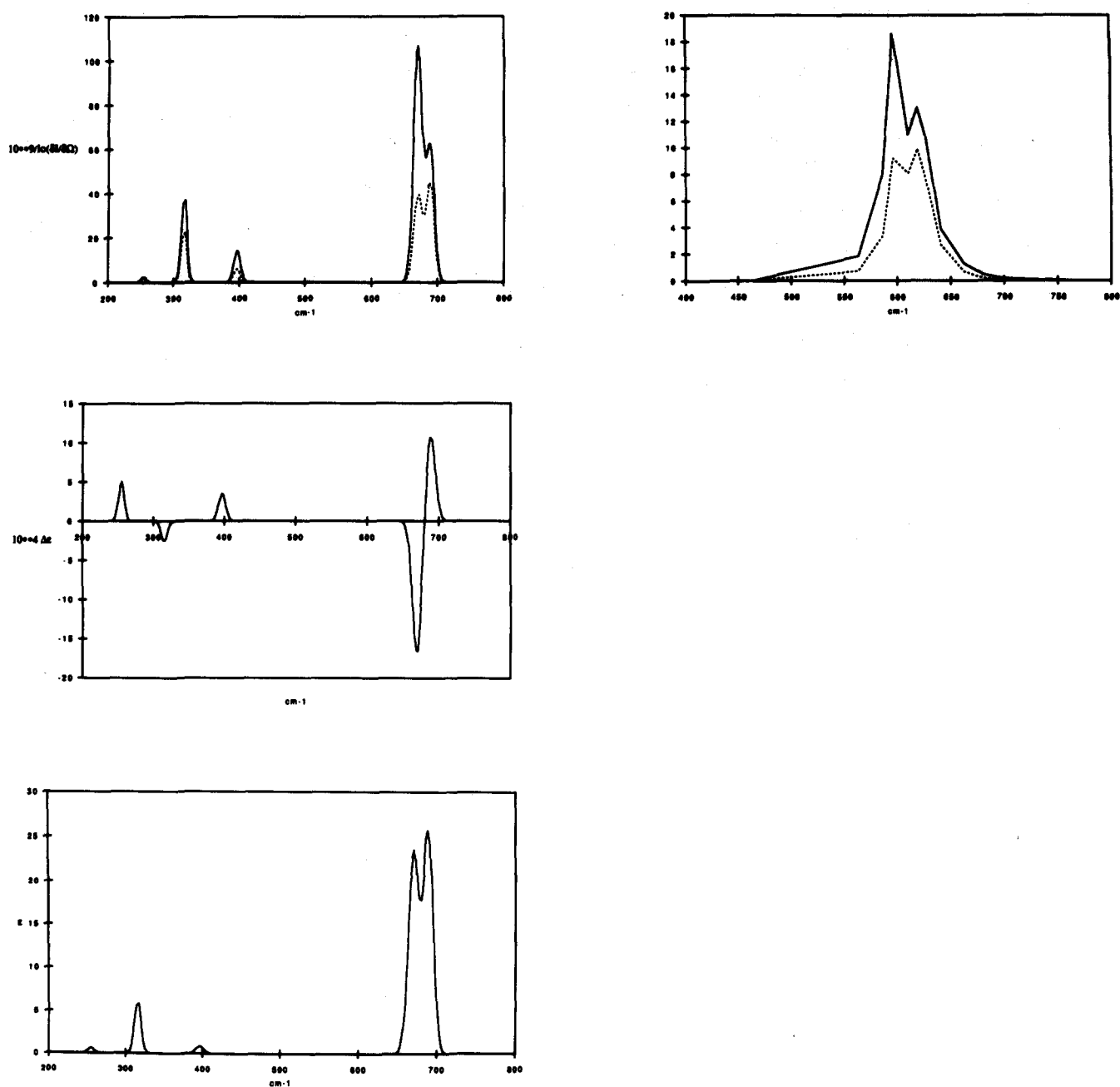| Q_i	$\bar{v}_i$	D_i	R_i(a)	R_i(b)	R_i(c)	$10^4 g_i$(a)	σ_i^P	σ_i^D
(CH$_3$)$_t$	255	1.599	3.230	2.432	3.086	8.08	0.078	0.058
(CH$_3$)$_i$	316	15.173	− 1.614	− 7.684	− 5.780	− 0.43	1.780	1.068
C–CH$_3$	396	2.147	2.171	3.951	4.250	4.04	1.066	0.445
Ring$_s$	670	49.264	− 9.088	− 3.547	− 9.926	− 0.74	20.389	7.436
Ring$_a$	688	53.593	5.801	− 2.387	9.846	0.43	12.277	8.924

FIG. 6. Raman experimental spectrum (right) of R-methylthiirane in the low-frequency (400–800 cm^{-1}) region; the theoretical spectra (left) have been computed in the frequency interval 250–700 cm^{-1} by the MP2 method. IR (lower), VCD (middle), polarized (full line), and depolarized (dashed line) Raman spectra (upper). Gauge, scaling factors, and units for the theoretical intensities as in Fig. 1. The experimental Raman intensities from Ref. 23 are given in arbitrary units.

ACKNOWLEDGMENTS

[1] For general definitions, see *Vibrational Intensities in Infrared and Raman Spectroscopy,* edited by W. B. Person and G. Zerbi (Elsevier, Amsterdam, 1982).

[2] J. A. Koningstein, *Introduction to the Theory of the Raman Effect* (Reidel, Dordrecht, Holland, 1971).

[3] P. J. Stephens and M. A. Lowe, Annu. Rev. Phys. Chem. **36**, 213 (1985).

[4] L. A. Nafie, J. Chem. Phys. **79**, 4950 (1983).

[5] A. D. Buckingham, P. W. Fowler, and P. A. Galwas, Chem. Phys. **112**, 1 (1987).

[6] P. J. Stephens, J. Phys. Chem. **89**, 748 (1985).

[7] L. Nafie, *Advances in Infrared and Raman Spectroscopy,* edited by R. J. H. Clark and R. E. Hester (Heyden, London, 1984), Vol. 11, p. 49.

[8] S. F. Mason, in Ref. 7, p. 283.

[9] D. P. Craig and T. Thirunamachandran, Mol. Phys. **35**, 825 (1978).

[10] P. Lazzeretti, R. Zanasi, and P. J. Stephens, J. Phys. Chem. **90**, 6761 (1986).

[11] R. D. Amos, N. C. Handy, A. F. Drake, and P. Palmieri, J. Chem. Phys. **89**, 7287 (1988).

[12] M. A. Lowe, P. J. Stephens, and G. A. Segal, Chem. Phys. Lett. **123**, 108 (1986).

[13] M. A. Lowe, G. A. Segal, and P. J. Stephens, J. Am. Chem. Soc. **108**, 248 (1986).

[14] R. D. Amos, N. C. Handy, K. J. Jalkanen, and P. J. Stephens, Chem. Phys. Lett. **133**, 21 (1988).

[15] K. J. Jalkanen, P. J. Stephens, R. D. Amos, and N. C. Handy, Chem.

[15] Phys. Lett. **142**, 153 (1987).

[16] M. A. Lowe, J. S. Alper, R. W. Kawiecki, and P. J. Stephens, J. Phys. Chem. **90**, 41 (1986).

[17] K. Morokuma and H. Segeta, Chem. Phys. Lett. **134**, 23 (1987).

[18] R. D. Amos, Adv. Chem. Phys. **67**, 99 (1987).

[19] For a recent review on this field, see B. A. Hess, Jr., L. J. Schaad, P. Carski, and R. Zaharadnik, Chem. Rev. **86**, 709 (1986).

[20] P. Pulay, G. Fogarasi, and J. E. Boggs, J. Chem. Phys. **74**, 3999 (1981).

[21] C. E. Blom and C. Altona, Mol. Phys. **31**, 1377 (1976).

[22] C. E. Blom and A. Müller, J. Mol. Spectrosc. **70**, 449 (1978).

[23] P. L. Polavarapu, B. A. Hess, Jr., L. J. Schaad, D. O. Henderson, L. P. Fontana, H. E. Smith, L. A. Nafie, T. B. Freedman, and W. M. Zuk, J. Chem. Phys. **86**, 1140 (1987).

[24] H. Dothe, M. A. Lowe, and J. S. Alper, J. Phys. Chem. **92**, 6246 (1988).

[25] P. K. Bose and P. L. Polavarapu, Chem. Phys. Lett. **152**, 39 (1988).

[26] C. Møller and M. S. Plesset, Phys. Rev. **46**, 618 (1934).

[27] J. S. Binkley and J. A. Pople, Int. J. Quantum Chem. **9**, 229 (1975).

[28] R. D. Amos and J. E. Rice, "The Cambridge Analytic Derivatives Package," Cambridge, U.K., 1987.

[29] T. H. Dunning, Jr., J. Chem. Phys. **53**, 2833 (1970).

[30] W. J. Hehre, R. Ditchfield, and J. A. Pople, J. Chem. Phys. **54**, 724 (1971).

[31] The 6-31G-extended basis is produced by adding one extra shell of each type to the 6-31G** basis. In the present case, the types and exponents of the additional functions are: for hydrogen, s, 0.054 and p, 0.25; for carbon, s, 0.056; p, 0.056; and d, 0.266; and for sulphur, s, 0.039; p, 0.039; and d, 0.22.

[32] W. S. Brickell, S. F. Mason, and D. R. Roberts, J. Chem. Soc. B **1971**, 691.

[33] S. F. Mason and R. H. Seal, Tetrahedron **30**, 1671 (1974).

[34] P. J. Stephens, J. Phys. Chem. **91**, 1712 (1987).

[35] D. P. Craig and T. Thirunamachandran, Can. J. Chem. **63**, 1773 (1985).

[36] L. Nafie, P. L. Polavarapu, and M. Diem, J. Chem. Phys. **73**, 3530 (1980).